High-T_g TOPAS microstructured polymer optical fiber for fiber Bragg grating strain sensing at 110 degrees

Christos Markos,[1,2,6] Alessio Stefani,[2,4] Kristian Nielsen,[2] Henrik K. Rasmussen,[3] Wu Yuan,[2,5] and Ole Bang[2,*]

[1]*Department of Computer Engineering and Informatics, University of Patras, Patra, 26500, Greece*
[2]*DTU Fotonik, Department of Photonics Engineering, Technical University of Denmark, DK-2800 Kgs. Lyngby, Denmark*
[3]*Department of Mechanical Engineering, Technical University of Denmark, DK-2800 Kgs. Lyngby, Denmark*
[4]*Max Planck Institute for the Science of Light, Guenter-Scharowsky Str. 1, 91058 Erlangen, Germany*
[5]*Singapore Institute of Manufacturing Technology, 71 Nanyang Drive, 638075, Singapore*
[6]*Theoretical and Physical Chemistry Institute, National Hellenic Research Foundation, Athens, 11635, Greece*
[*]*oban@fotonik.dtu.dk*

Abstract: We present the fabrication and characterization of fiber Bragg gratings (FBGs) in an endlessly single-mode microstructured polymer optical fiber (mPOF) made of humidity-insensitive high-Tg TOPAS cyclic olefin copolymer. The mPOF is the first made from grade 5013 TOPAS with a glass transition temperature of Tg = 135°C and we experimentally demonstrate high strain operation (2.5%) of the FBG at 98°C and stable operation up to a record high temperature of 110°C. The Bragg wavelengths of the FBGs are around 860 nm, where the propagation loss is 5.1dB/m, close to the fiber loss minimum of 3.67dB/m at 787nm.

OCIS codes: (060.2370) Fiber optics sensors; (060.4005) Microstructured fibers; (350.2770) Gratings; (060.2270) Fiber characterization; (160.5470) Polymers.

References and links

1. J. B. Jensen, P. E. Hoiby, G. Emiliyanov, O. Bang, L. H. Pedersen, and A. Bjarklev, "Selective detection of antibodies in microstructured polymer optical fibers," Opt. Express **13**(15), 5883–5889 (2005).
2. A. Dupuis, N. Guo, Y. Gao, N. Godbout, S. Lacroix, C. Dubois, and M. Skorobogatiy, "Prospective for biodegradable microstructured optical fibers," Opt. Lett. **32**(2), 109–111 (2007).
3. F. M. Cox, A. Argyros, and M. C. J. Large, "Liquid-filled hollow core microstructured polymer optical fiber," Opt. Express **14**(9), 4135–4140 (2006).
4. G. Emiliyanov, J. B. Jensen, O. Bang, P. E. Hoiby, L. H. Pedersen, E. M. Kjaer, and L. Lindvold, "Localized biosensing with Topas microstructured polymer optical fiber," Opt. Lett. **32**(5), 460–462 (2007).
5. G. Emiliyanov, J. B. Jensen, O. Bang, P. E. Hoiby, L. H. Pedersen, E. M. Kjaer, and L. Lindvold, "Localized biosensing with TOPAS microstructured polymer optical fiber: Erratum," Opt. Lett. **32**(9), 1059 (2007).
6. F. M. Cox, A. Argyros, M. C. J. Large, and S. Kalluri, "Surface enhanced Raman scattering in a hollow core microstructured optical fiber," Opt. Express **15**(21), 13675–13681 (2007).
7. C. Markos, W. Yuan, K. Vlachos, G. E. Town, and O. Bang, "Label-free biosensing with high sensitivity in dual-core microstructured polymer optical fibers," Opt. Express **19**(8), 7790–7798 (2011).
8. A. Cusano, A. Cutolo, and J. Albert, *Fiber Bragg Grating Sensors: Recent Advancements, Industrial Applications and Market Exploitation* (Bentham Science Publishers, 2009), Chap. 15.
9. A. Stefani, S. Andresen, W. Yuan, N. Herholdt-Rasmussen, and O. Bang, "High Sensitivity Polymer Optical Fiber-Bragg-Grating-Based Accelerometer," IEEE Photon. Technol. Lett. **24**(9), 763–765 (2012).
10. Z. Xiong, G. D. Peng, B. Wu, and P. L. Chu, "Highly tunable Bragg gratings in single-mode polymer optical fibers," IEEE Photon. Technol. Lett. **11**(3), 352–354 (1999).
11. H. Dobb, D. J. Webb, K. Kalli, A. Argyros, M. C. J. Large, and M. A. van Eijkelenborg, "Continuous wave ultraviolet light-induced fiber Bragg gratings in few- and single-mode microstructured polymer optical fibers," Opt. Lett. **30**(24), 3296–3298 (2005).
12. I. P. Johnson, K. Kalli, and D. J. Webb, "827 nm Bragg grating sensor in multimode microstructured polymer optical fibre," Electron. Lett. **46**(17), 1217–1218 (2010).
13. A. Stefani, W. Yuan, C. Markos, and O. Bang, "Narrow bandwidth 850 nm fiber Bragg gratings in few-mode polymer optical fibers," IEEE Photon. Technol. Lett. **23**(10), 660–662 (2011).

#183057 - $15.00 USD Received 8 Jan 2013; revised 13 Feb 2013; accepted 13 Feb 2013; published 19 Feb 2013

14. M. A. van Eijkelenborg, M. C. J. Large, A. Argyros, J. Zagari, S. Manos, N. A. Issa, I. Bassett, S. Fleming, R. C. McPhedran, C. M. de Sterke, and N. A. P. Nicorovici, "Microstructured polymer optical fibre," Opt. Express **9**(7), 319–327 (2001).
15. T. Ishigure, M. Hirai, M. Sato, and Y. Koike, "Graded-index plastic optical fiber with high mechanical properties enabling easy network installations. I," J. Appl. Polym. Sci. **91**(1), 404–409 (2004).
16. A. Argyros, R. Lwin, S. G. Leon-Saval, J. Poulin, L. Poladian, and M. C. J. Large, "Low loss and temperature stable microstructured polymer optical fibers," J. Lightwave Technol. **30**(1), 192–197 (2012).
17. K. E. Carroll, C. Zhang, D. J. Webb, K. Kalli, A. Argyros, and M. C. J. Large, "Thermal response of Bragg gratings in PMMA microstructured optical fibers," Opt. Express **15**(14), 8844–8850 (2007).
18. C. Zhang, W. Zhang, D. J. Webb, and G. D. Peng, "Optical fibre temperature and humidity sensor," Electron. Lett. **46**(9), 643–644 (2010).
19. W. Yuan, A. Stefani, M. Bache, T. Jacobsen, B. Rose, N. Herholdt-Rasmussen, F. K. Nielsen, S. Andresen, O. B. Sørensen, K. S. Hansen, and O. Bang, "Improved thermal and strain performance of annealed polymer optical fiber Bragg gratings," Opt. Commun. **284**(1), 176–182 (2011).
20. W. Yuan, A. Stefani, and O. Bang, "Tunable polymer Fiber Bragg Grating (FBG) inscription: Fabrication of dual-FBG temperature compensated polymer optical fiber strain sensors," IEEE Photon. Technol. Lett. **24**(5), 401–403 (2012).
21. I. P. Johnson, D. J. Webb, K. Kalli, M. C. J. Large, and A. Argyros, "Multiplexed FBG sensor recorded in multimode microstructured polymer optical fibre," Proc. SPIE **7714**, 77140D, 77140D-10 (2010).
22. K. Makino, T. Kado, A. Inoue, and Y. Koike, "Low loss graded index polymer optical fiber with high stability under damp heat conditions," Opt. Express **20**(12), 12893–12898 (2012).
23. G. Khanarian, "Optical properties of cyclic olefin copolymers," Opt. Eng. **40**(6), 1024–1029 (2001).
24. W. Yuan, L. Khan, D. J. Webb, K. Kalli, H. K. Rasmussen, A. Stefani, and O. Bang, "Humidity insensitive TOPAS polymer fiber Bragg grating sensor," Opt. Express **19**(20), 19731–19739 (2011).
25. I. P. Johnson, W. Yuan, A. Stefani, K. Nielsen, H. K. Rasmussen, L. Khan, D. J. Webb, K. Kalli, and O. Bang, "Optical fibre Bragg grating recorded in TOPAS cyclic olefin copolymer," Electron. Lett. **47**(4), 271–272 (2011).
26. K. Nielsen, H. K. Rasmussen, A. J. L. Adam, P. C. M. Planken, O. Bang, and P. U. Jepsen, "Bendable, low-loss Topas fibers for the terahertz frequency range," Opt. Express **17**(10), 8592–8601 (2009).
27. S. Atakaramians, S. Afshar V., M. Nagel, H. K. Rasmussen, O. Bang, T. M. Monro, and D. Abbott, "Direct probing of evanescent field for characterization of porous terahertz fibers," Appl. Phys. Lett. **98**(12), 121104 (2011).
28. H. Bao, K. Nielsen, H. K. Rasmussen, P. U. Jepsen, and O. Bang, "Fabrication and characterization of porous-core honeycomb bandgap THz fibers," Opt. Express **20**, 29507–29517 (2012).
29. See, *www.topas.com*
30. A. Stefani, K. Nielsen, H. K. Rasmussen, and O. Bang, "Cleaving of TOPAS and PMMA microstructured polymer optical fibers: Core-shift and statistical quality optimization," Opt. Commun. **285**(7), 1825–1833 (2012).
31. M. C. J. Large, L. Poladian, G. Barton, and M. A. van Eijkelenborg, *Microstructured Polymer Optical Fibres* (Springer, 2008).

1. Introduction

Polymer optical fibers (POFs) have several advantages compared to silica fibers. First of all, POFs can be used for clinical applications due to their biocompatibility, which combined with their flexibility and non-brittle nature makes them a potential platform for in-vivo biosensing applications [1–7]. Two other important properties of POFs are their high failure strain, which makes them suitable for high strain (above 1%) sensing applications [8], and the low Young's modulus (30 times lower than silica), making the POFs more sensitive to displacement forces [8, 9]. The first polymer FBG sensor was a 1576 nm FBG fabricated in a photosensitive polymethylmethacrylate (PMMA) single-mode step-index POF in 1999 [10], whereas the first FBG written in a single-mode microstructured POF (mPOF), was a 1570 nm grating reported in 2005 [11]. It was first about 5 years later that FBGs at around 850 nm, where the mPOFs have lower loss, were reported [12, 13]. Traditionally, POFs, mPOFs, and polymer FBGs have been made of PMMA [1, 3, 6, 10–21], which makes the response of the FBGs dependent on both temperature and humidity [17–21]. This fact, together with the issue of high loss and low operating temperature, has been hindering the application of polymer FBGs in key strain sensing and biosensing areas [8].

The environmental conditions can be compensated for with the dual-grating technology, where only one FBG is subjected to strain [20, 21]. Although progress has been made towards reducing the influence of humidity on PMMA fibers by doping [22], the issue of humidity

#183057 - $15.00 USD Received 8 Jan 2013; revised 13 Feb 2013; accepted 13 Feb 2013; published 19 Feb 2013

dependency was first solved with the fabrication of the first TOPAS mPOF in 2007 [4, 5]. The polymer TOPAS belongs to the class of cyclic olefin copolymers (COCs), which is a class of optical thermoplastics that are chemically inert and have a very low moisture uptake, high water barrier, and good optical transmission [23]. This means that a TOPAS FBG is humidity insensitive [24]. However, the aim with the original fiber was to use the chemical inertness of TOPAS for localized fluorescence-based biosensing [4, 5]. It was first in 2011 that a 1569 nm FBG was written into a TOPAS mPOF, using 325 nm UV writing [25]. Soon thereafter an 871 nm FBG in a TOPAS mPOF was reported and it was demonstrated that the TOPAS FBG was indeed humidity insensitive to within the accuracy of the climate chamber that was used [24]. Interestingly, it has been demonstrated that TOPAS is also a very good material for terahertz (THz) fiber fabrication due to its low material loss and material dispersion at THz frequencies [26–28].

In all published papers on TOPAS mPOFs, the fibers were made of the particular TOPAS grade 8007, which has a glass transition temperature of only T_g = 80°C [29]. This is even lower than that of PMMA (typically 110°C), which means that the issue of a low operating temperature remains a problem for polymer FBGs. Here we demonstrate for the first time the fabrication of an mPOF made of high-T_g TOPAS grade 5013 with T_g = 135°C. We further inscribe FBGs into the fiber and demonstrate strain sensing of 2.5% strain at 98°C, where a PMMA fiber would malfunction (max. operation temperature of 92°C demonstrated in [17]). Further we also demonstrate strain sensing at a record high temperature of 110°C. Due to setup limitations the strain sensing at 110°C is limited to strains up to 0.3%. For applications in for example accelerometers, the strain rarely exceeds 0.3% [9].

Taking into consideration that the TOPAS fiber is humidity insensitive [24] and that the TOPAS FBG strain sensor may be temperature compensated using dual-FBG technology [20, 21], this demonstration of high-temperature operation at 110 °C provides a significant step towards a practically applicable polymer FBG sensor platform. The fiber is shown to have a minimum loss of 3.67 dB/m at 787 nm and a loss of 5.1 dB/m at the FBG wavelength 853 nm.

2. Experimental results

2.1 Fabrication of high-Tg TOPAS mPOF and FBG inscription

In our experiments we employed a high-Tg TOPAS mPOF fabricated in-house at DTU Fotonik using the drill and draw technique. The material used for the mPOFs was TOPAS COC of the particular grade 5013, obtained from TOPAS Advanced Polymers, Inc. The TOPAS was cast into 6 cm diameter rod and the desired hexagonal holes structure was drilled into the rod. The preforms were then drawn to fiber by first drawing a 5 mm cane, which was then sleeved and drawn again. The two final high-T_g TOPAS mPOFs we use here have a diameter of 130 μm and 180 μm, respectively, and a solid core surrounded by three rings of air holes arranged in a hexagonal lattice. For the fiber with a diameter of 130 μm the air-hole diameter is $d = 2.2 \pm 0.2$ μm and the distance between the air-holes (pitch) is on average Λ = 6 μm, which means that the fiber is endlessly single moded ($d/\Lambda < 0.43$). The end facet of the high-Tg fiber with a diameter of 130 μm is shown in the inset of Fig. 1(a).

The grating inscription was performed using a 30 mW CW HeCd laser operating at 325 nm (IK5751I-G, Kimmon). A circular Gaussian laser beam was expanded by a cylindrical lens in one direction, the one along the fiber, from 1.2 mm to 1.2 cm. The laser beam was then focused downwards using another cylindrical lens to sideways expose the core of the fiber through a phase-mask. The phase mask has been custom made for 325 nm writing with a uniform period of 572.4 nm (Ibsen Photonics). This would result in a Bragg grating wavelength λ_B of 872 nm if no annealing or pre-strain was applied. However, depending on the applied pre-strain and thermal treatment of the fiber the grating resonance will be blue-shifted [20, 21]. As an example the final grating wavelength of the fiber with a diameter of

#183057 - $15.00 USD Received 8 Jan 2013; revised 13 Feb 2013; accepted 13 Feb 2013; published 19 Feb 2013

130 μm was 853.4 nm and the strength of the reflected peak was around 20 dB, as shown in Fig. 1(a). The about 19 nm blue-shift is because we both used pre-strain and afterwards annealed the FBG.

Since the TOPAS high-T_g optical grade 5013 mPOF was not reported before, a cut-back measurement with 5 cuts was performed in order to determine the transmission loss of the fiber. Cleaving was done with a homemade electronically controlled hot blade cleaver with flat side blade at a temperature of 75°C for both the blade and fiber, giving a high quality cleaves [30]. Figure 1(b) shows the loss profile of the high-Tg TOPAS mPOF for the wavelength span of 500-1000 nm. The loss at the Bragg wavelength 853.4 nm is found to be 5.12 dB/m, whereas the minimum loss is 3.67 dB/m at 787 nm. The loss can be reduced by optimizing the drawing process [16], but in our experiments the loss is not a limiting factor.

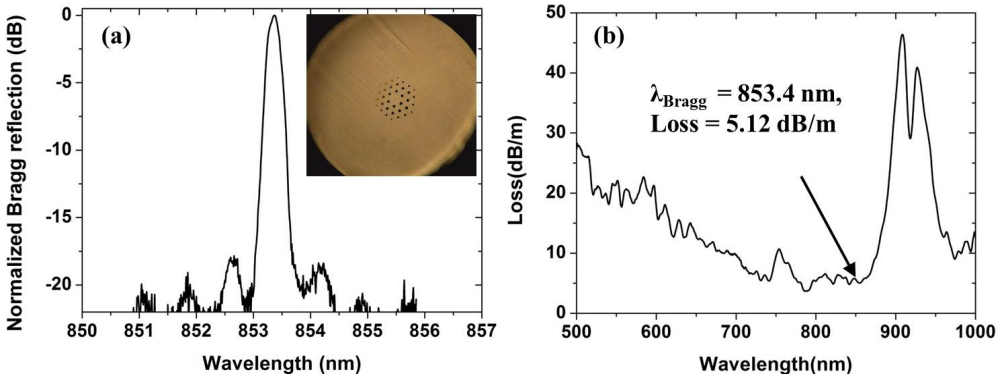

Fig. 1. (a) Reflection spectrum of the high-T_g TOPAS FBG at room temperature. Inset: microscope image of the end fact of the mPOF (130 μm in diameter) with a 3-ring hexagonal holes structure. (b) Measured loss of the fiber.

2.2 Thermal response of high-T_g mPOF FBGs

The temperature response of the grating of the 130 μm fiber shown in Fig. 1(a) was studied by monitoring the reflection spectrum using a fiber circulator, a supercontinuum source (SuperK Versa by NKT Photonics A/S) and an optical spectrum analyzer (Ando AQ6317B). Light was launched into the mPOF using a silica step index fiber, which was butt-coupled to the mPOF. In order to reduce the background noise, a small amount of refractive index matching gel was applied between the silica fiber and the mPOF to minimize Fresnel reflections. The grating was then placed on a resistive hot stage to control the temperature. A thermocouple was placed as close to the grating as possible with a temperature uncertainty of 2%, while several layers of lens paper were covering the grating to isolate it and create a more uniform temperature. For stable strain sensing it is crucial to anneal the fiber before operation [17, 19]. We therefore annealed the FBGs for ~3 hours at 80 degrees before operation.

#183057 - $15.00 USD Received 8 Jan 2013; revised 13 Feb 2013; accepted 13 Feb 2013; published 19 Feb 2013

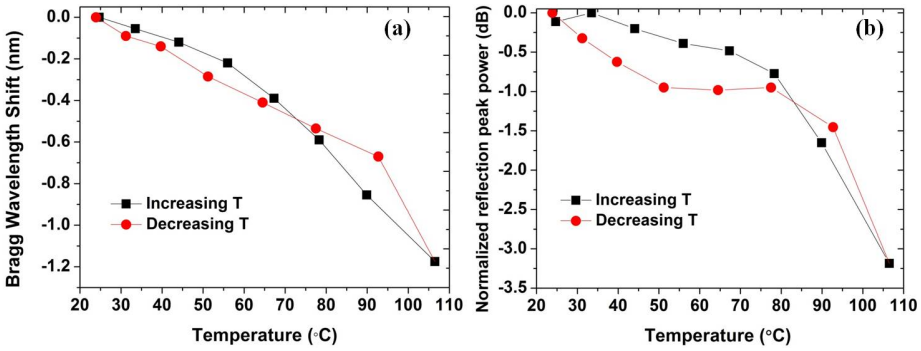

Fig. 2. Temperature response of the FBG in the 130 μm fiber shown in Fig. 1. (a) Bragg wavelength shift versus temperature. (b) Normalized reflected peak power versus temperature.

Figure 2(a) shows how the Bragg wavelength blue-shifts by 1.2 nm as the temperature is increased to 107°C, waiting 20 minutes at each temperature for the fiber to stabilize before making a recording. Only a very small hysteresis is observed, while the wavelength shift is returning to zero as the temperature is ramped down again at 20 minute intervals, which indicates that the fiber was properly annealed before operation. Figure 2(b) shows the reflected normalized power at the (temperature dependent) Bragg wavelength. The power returns also to the initial level after a full temperature cycle, but fluctuations are apparent and a maximum hysteresis of 0.75dB occurs at 50°C. The small power variation between the forward and reverse temperature cycle is probably due to experimental errors, such as laser fluctuation, coupling instabilities, etc. The total drop of the reflected power is 3.2 dB at the maximum temperature of 107°C.

2.3 Small strain response of high-T_g mPOF FBGs under different temperatures

The small strain response of the FBG in the 130 μm in diameter high-T_g TOPAS mPOF was investigated by mechanical stretching. The two ends of the fiber were clamped and glued to two micro-translation stages (Thorlabs) with UV-cured glue, with one of them used to butt-couple the mPOF to the single-mode silica fiber. The glue is mechanically much stiffer than the high-Tg TOPAS mPOF, so that it does not unduly influence the strain. One stage can move longitudinally to apply axial strain to the grating manually with a low loading speed. The axial strain values were determined by dividing the fiber longitudinal elongation by the length of fiber between the two gluing points. The gratings were left to stabilize for about ten minutes at each value of the strain, before a recording was made.

#183057 - $15.00 USD Received 8 Jan 2013; revised 13 Feb 2013; accepted 13 Feb 2013; published 19 Feb 2013

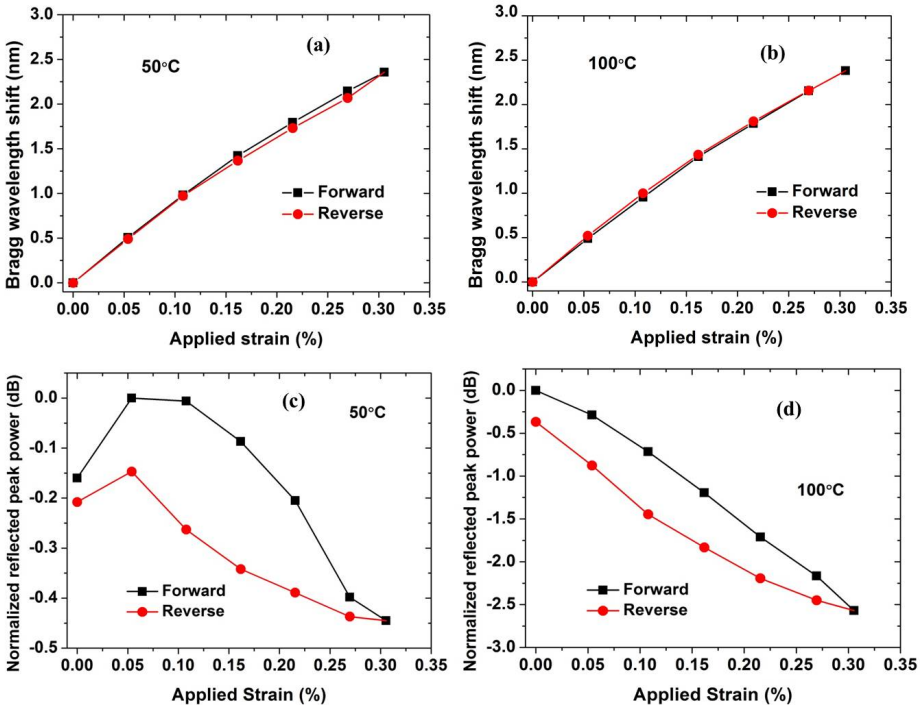

Fig. 3. Small strain response of the FBG in the 130 μm fiber shown in Fig. 1. (a-b) Bragg wavelength shift vs strain at (a) 50°C and (b) 100°C. (c-d) Corresponding normalized reflected peak power for (c) 50°C and (d) 100°C. Red lines show strain loading, whereas black lines show subsequent strain release. At each strain value the grating is left for 10 minutes before a recording is made.

Figures 3(a) and (b) show the Bragg wavelength shift versus strain for a complete strain loading and release cycle to over 0.3% and back, for operation at 50°C and 100°C, respectively. The grating shows almost a linear response of the wavelength shift over the whole strain loading range and a linear fit of the results give a slope of 0.76 pm/με at 50°C and 0.80 pm/με at 100°C. Figures 3(c) and (d) show the corresponding drop of the peak power at the same temperatures. At 50°C the peak power varies only by 0.45 dB, while at 100°C, the power is reduced by about 2.5 dB. From Fig. 2(b) we see that the 2.5 dB drop corresponds well with the drop due to temperature alone. Again the small power variation between the forward and reverse strain loading cycle is probably due to experimental errors, such as laser fluctuation, coupling instabilities, etc.

PMMA FBGs have been taken to 92°C without applied strain [17] and here the high-Tg TOPAS mPOF survived 100°C at 0.3% strain, which is clearly a record. A golden rule for long term stability is to keep the temperature at least 20°C below the glass-transition temperature. PMMA has a T_g around 110°C, so a PMMA FBG could therefore in principle survive 100°C for a short time. Our high-T_g TOPAS has a T_g of 135°C, so we therefore finally test our 130 μm FBG for small strain operation at 110°C. The Bragg wavelength shift for a strain loading-unloading cycle is shown in Fig. 4(a) giving a slope of 1.0 pm/με. In order for the Bragg wavelength to be recoverable and avoid destroying the grating the operational strain regime of the FBG was kept below 0.16%, where the peak power has decreased by 6 dB as shown in Fig. 4(b). We note that 0.16% is still significantly more than the 0.02% used in the recent demonstration of highly sensitive mPOF FBG accelerometers taken to 15 g [9].

#183057 - $15.00 USD Received 8 Jan 2013; revised 13 Feb 2013; accepted 13 Feb 2013; published 19 Feb 2013

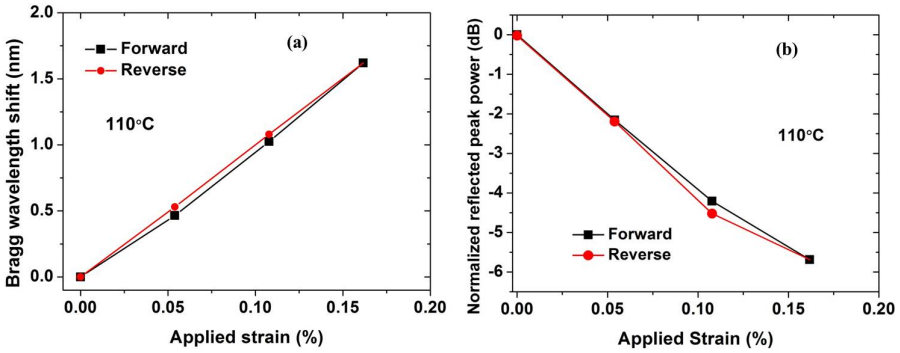

Fig. 4. Small strain response of the FBG in the 130 µm fiber shown in Fig. 1. (a) Bragg wavelength shift vs strain at 110°C. (b) Corresponding normalized reflected peak power. Red lines show strain loading, whereas black lines show subsequent strain release. At each strain value the grating is left for 10 minutes before a recording is made.

2.4 Time response of high-T_g mPOF FBGs at 110°C

In this section, we demonstrate the thermal stability of the 130 µm in diameter mPOF FBG made of high-T_g TOPAS mPOF at 110°C. In this measurement one end of the fiber was glued to a stage and used for incoupling, while the other end of the fiber was not mounted to avoid unwanted strain. Figure 5(a) shows the blue-shift of the Bragg grating with time while the variation of the Bragg wavelength shift is shown in Fig. 5(b). The total shift of the resonant wavelength was 5 nm after 7 hours at 110°C. After 7 hours the temperature was decreased to room temperature and after 17 hours at room temperature the resonant wavelength did not recover, but remained at the same wavelength.

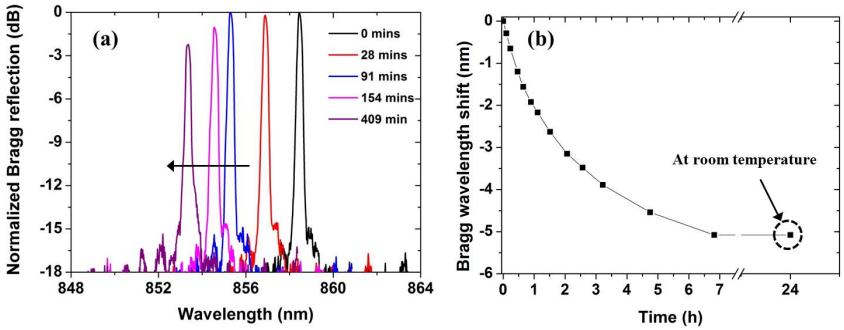

Fig. 5. (a) Normalized Bragg grating reflection spectrum indicating the blue-shift of the resonant wavelength. (b) The variation of Bragg wavelength with time at 110°C. After 17 hours at room temperature, the Bragg wavelength remains at the same position as after 7 hours at 110°C.

This permanent blue-shift of the resonant wavelength can be explained by fiber shrinking. The polymer optical fibers are pulled under tension, which results in an axial orientation of the polymer chains and a residual strain in the fiber [8, 31]. At a certain temperature the chains relax from the axial orientation, which causes shrinkage of the fiber. This effect is directly linked with the drawing tension, thermal history and the annealing process of the fiber and has been extensively studied [8, 31]. The blue-shift indicates that possibly the high-T_g TOPAS FBGs would benefit from being annealed for a longer time than 3 hours at 80°C or at a higher temperature. However, an investigation into the optimum annealing time and temperature for the high-T_g TOPAS FBG is outside the scope of this initial demonstration of fiber drawing, FBG writing, and high-temperature operation.

#183057 - $15.00 USD Received 8 Jan 2013; revised 13 Feb 2013; accepted 13 Feb 2013; published 19 Feb 2013

2.5 Large strain response of high-T_g mPOF FBGs under different temperatures

Although in many applications only small strains are needed [9], polymer fibers are superbly well suited in applications where large strains are needed, such as in geo-textiles monitoring land-slides and in respiratory monitoring, due to their high failure strain [8]. In this section the large strain response of the high-T_g TOPAS FBG is investigated. Using the same setup as in the low strain section and, a similar fiber, 180 μm in diameter with a hole diameter around 3 μm and a pitch around 8 μm, is subjected to strains up to 3% at room temperature, 2.2% at 50°C and 2.5% at 98°C. The Bragg grating wavelength of the unstrained fiber was 869.6 nm. The gratings were left to stabilize for about two minutes at each level of applied strain. The result of this strain investigation is shown in Fig. 6.

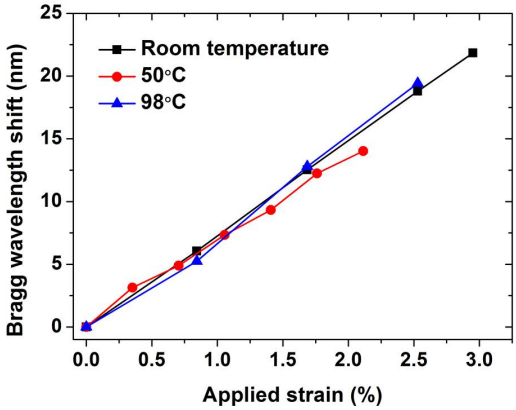

Fig. 6. Large strain response of the 180 μm TOPAS FBG at room temperature, 50°C, and 98°C

The gratings were strained until the glue holding the fiber failed. For this reason there is no data on the releasing of the strain. The large-strain response is also found to be approximately linear, with the grating response at 98°C having a fitted linear slope of 0.75 pm/με.

3. Conclusions

In this paper, we have demonstrated for the first time the response of FBGs inscribed in a new high-T_g TOPAS mPOF. The host material used for the fabrication of fiber was grade 5013 TOPAS cyclic olefin copolymer, which has a glass transition temperature as high as Tg = 135°C. We demonstrate that FBGs in the high-T_g TOPAS mPOF are able to operate at 110°C under applied tensile strain up to 0.16% and at 98°C under applied tensile strain up to 2.5%. It should be emphasized that there is not any report so far demonstrating the operation of PMMA POFs or mPOFs at higher temperature than 92°C [17]. The fiber was characterized under applied tensile strain at 50°C, 100°C and 110°C demonstrating consistent repeatability for all cases. We also investigated the thermal stability of the FBGs over time. The fiber was heated for around 7 hours at 110°C with a total resonant wavelength blue-shift of ~5 nm. It should be mentioned that after 24 hours at room temperature, the resonant Bragg wavelength remained at the same position. Overall, we believe that the current work is a significant step towards fabrication and commercialization of polymer FBG sensors based on TOPAS, which further enhances the ability of polymer fibers to operate at temperatures up to 110°C.

Acknowledgments

The authors acknowledge support from the IntelliCIS COST Action IC0806.

#183057 - $15.00 USD Received 8 Jan 2013; revised 13 Feb 2013; accepted 13 Feb 2013; published 19 Feb 2013